International Journal of
INTELLIGENT SYSTEMS AND APPLICATIONS IN ENGINEERING
ISSN:2147-6799 www.ijisae.org Original Research Paper

PV Wind Based Stand-Alone Multi Input Electric Vehicle Charging Stations

Ramesh Jatoth[1], Srinivas cheera[2], B. Mangu[3], T. Murali Krishna[4]

Submitted: 10/08/2024 **Revised:** 30/08/2024 **Accepted :** 15/09/2024

Abstract*:* Operating renewable sources without grid support is considered to be crucial task as the load power compensation need stabilized voltage. In a grid connected renewable system the voltage stability and deficit power are compensated by the conventional grid. In the standalone renewable system, the voltages and generating power are unpredictable and unstable. In order to stabilize the voltage of the system an energy storage device need to be included. For efficient hybrid renewable power delivery, a multi-input transformer coupled active bridge converter is adopted. The proposed circuit topology has three input ports and one output port. From the three input ports, two are low voltage ports and one is medium voltage port. The low voltage ports are connected to PV panels, battery pack and medium voltage port is connected to wind energy source. All the sources share powers to the output port through HFTF compensating the AC load with an inverter. The primary side of HFTF has two active bridges each comprising a pair of high frequency operating MOSFET switches. These switches are controlled by MPPT and voltage regulator control modules as per the renewable power availability. On the secondary side of the HFTF an uncontrolled rectifier is connected along with a single-phase inverter for load compensation. Different operating conditions of the renewable sources are considered for the analysis of the proposed circuit topology. The performance analysis of the proposed system carried out in Simulink environment of the MATLAB software.

Keywords: *Multi-input transformer coupled active bridge converter, PV (Photo Voltaic), HFTF (High Frequency Transformer), MOSFET (Metal Oxide Field Effect Transistor), MPPT (Maximum Power Point Tracking), Simulink, MATLAB (Matrix Laboratory)*.

1. Introduction

Shifting of power generation from conventional fossil fuel sources to renewable sources is a critical task as the renewable sources are unstable and unreliable in a power system. When the grid system is integrated with renewable sources many uncertainties are caused creating power quality issues [1]. If the renewable sources are connected in parallel to the grid sharing renewable power in parallel with the conventional power the system is likely to be stable as the conventional source is reliable. But when the renewable source is connected in standalone system where no conventional source is available, there are many unstable conditions created in the system [2]. As the renewable sources depend on the available natural sources like winds, solar irradiation, tidal waves, biogas etc, the power generated by the sources is unpredictable as the natural sources. However, the renewable sources do not leave any carbon foot print as complete natural sources are used to generate electrical power.

In order to stabilize the voltages of the renewable sources in a standalone system (no grid connection) energy storage device (battery pack) is used [3]. The battery pack stores and delivers power to the system as per the renewable power availability maintaining the voltage magnitudes. In previous researches individual power circuits and controllers are used to for the renewable sources and the battery pack to ensure voltage stability. Conventional converters like boost and bidirectional converters are used for the voltage stabilization [4]. These converters have very high ripple and losses which causes harmonics and reduced efficiency in the system. As the renewable sources are in their initial development stage, the power conversion efficiency is in the range of 30 – 50 % considered to be very low.

With the lower efficiency of the conventional converters the power delivery to the load will be reduced further. Therefore, an efficient circuit topology is needed with multiple ports which can include multiple renewable sources and also the battery pack. In order to achieve efficient power extraction and reduced ripple voltage generation with multiple renewable sources, a ‘multi-input transformer coupled active bridge converter’ is adopted [5]. This converter has multiple active bridges connected to a HFTF which magnetically transfers powers to the secondary network at high frequency AC. At the input different renewable sources along with a battery pack are connected for voltage stability [6]. The outline structure of the ‘multi-input transformer coupled active bridge converter’ with different renewable sources and local load connected is presented in figure 1.

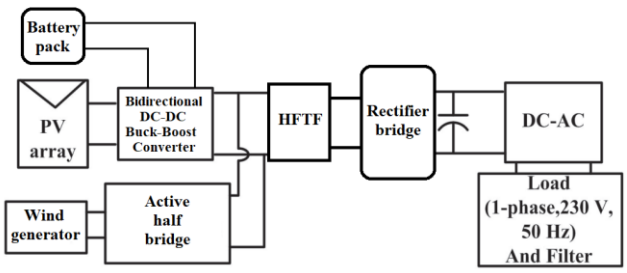

Figure 1: Multi-input transformer coupled active bridge converter topology outline

[1, 2, 3] *Department of Electrical Engineering, University College of Engineering(A), OU, Hyderabad*
[4] *Department of Electrical and Electronics Engineering, CBIT, Hyderabad*
ramesh.jatoth@gmail.com

In figure 1 the primary side of the HFTF two converters, 'Bidirectional DC-DC buck-boost converter' and 'Active half bridge' are connected in parallel. The bidirectional converter is included with 'PV array' and 'battery pack' which operate as per the available solar irradiation. On the DC link of the primary side HFTF a half active bridge is connected with wind generator connected to it [7]. The low voltages of the PV array and the battery pack are boosted by the bidirectional DC-DC buck boost converter and the voltage of the wind generator is boosted by the half active bridge. Both the converters are connected in parallel sharing power to the HFTF at high frequency AC.

On the secondary side of the HFTF a rectifier bridge is connected which converts the high frequency AC to DC through the diodes. The DC voltage generated at the output of the rectifier bridge has very low ripple content even at high power deliver conditions [8]. The reduced DC ripple voltage is converted to signal phase PWM (Pulse width Modulation) AC by a DC-AC full bridge inverter operated by Sin PWM technique. At the output of the inverter a LC filter is connected to ensure Sin AC voltage generation to the load connected. The LC filter mitigates the harmonics generated by the DC-AC full bridge inverter providing near to Sin voltage waveform to the load. Each converter has its own individual control module which defines the switching operating state as per the requirement. The initial PV array and battery pack converter is operated with respect to the MPPT algorithm and required DC link voltage. The wind generator connected half active bridge is controlled by MPPT of wind generator source. In any given condition the controllers tend to maintain the DC voltage at 400V which is converted to 230 – 240Vrms single phase AC voltage by the DC-AC inverter.

This paper is arranged with introduction to the proposed test system with multi renewable source standalone topology in section 1. The introduction includes the outline structure of the proposed multi-input transformer coupled active bridge converter topology and the modules connected to it. The following section 2 has the configuration of the proposed topology with its working principle and its mathematical derivations in different operating modes. The design of the controllers used for generating the switching pulses to the converters are included in section 3. The complete simulation and circuit analysis with different operating conditions is presented in section 4. The results sections include all the modules powers and voltages at different stage plotted with time as reference. The section 5 concludes the paper with validating the results determining the efficiency and advantages of the proposed topology compared to conventional methods. The reference cited in the paper are given after section 5.

2. Proposed circuit topology

As previously mentioned, the proposed topology 'multi-input transformer coupled active bridge converter' has three sources connected for power sharing to the load. The renewable sources are PV array, wind generator and the energy storage unit is a battery pack which charges or discharges as per the load demand and renewable power generated. The renewable sources are unidirectional sources which only generate power as per the natural source availability [9]. Therefore, both the renewable sources need only unidirectional converter for boosting the voltage as per the requirement. However, as the battery pack need to be charged during excess power and low SOC (State of Charge) condition it needs bidirectional converter. All the sources and storage unit are connected to a common DC link for power sharing to the load through the active bridge HFTF circuit [10]. The complete circuit structure of the 'multi-input transformer coupled active bridge converter' with single phase inverter included is presented in figure 2.

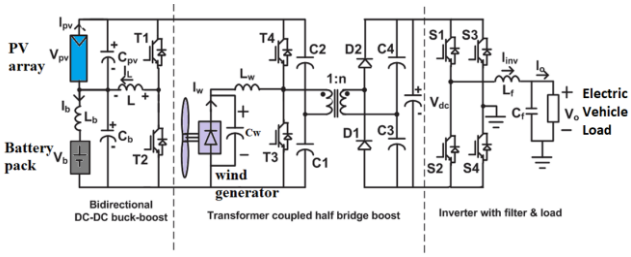

Figure 2: Proposed topology circuit diagram

In the given circuit figure 2 the PV array and the battery pack is connected to a common 'Bidirectional DC-DC buck boost converter' which extracts maximum power from connected PV panels. Along with the PV power extraction, the battery pack is current direction is also controlled by the same converter. This PV array and battery currents are controlled by the duty ratio variation of the IGBT switches T1 and T2. Here T1 is the boost switch for the PV array and buck switch of the battery pack and T2 is the boost switch for the battery pack. Both the switches T1 and T2 are operated alternatively through a NOT gate in order to avoid short circuit [11]. The low voltages of the PV array and the battery pack are boost to higher voltages with a gain of 2 - 2.5 times of the input voltage.

The DC link output of the bidirectional converter is connected to a half active half bridge with switches T3 and T4. These switches T3 and T4 also operated alternatively with a NOT gate logic to create AC voltage. Here, at the active bridge a wind generator module is connected with a PMSG machine connected to a diode bridge rectifier. The T3 switch of the active half bridge acts as boost switch to the wind generator module increasing the voltage output of the wind generator as per the system requirement. The boost voltage from all the source modules is converted to high frequency square wave AC by the active half bridge [12]. The high frequency AC is fed to HFTF for transferring power to the secondary side. The current conduction mode during the T3 ON state (negative conduction state) is presented in figure 3.

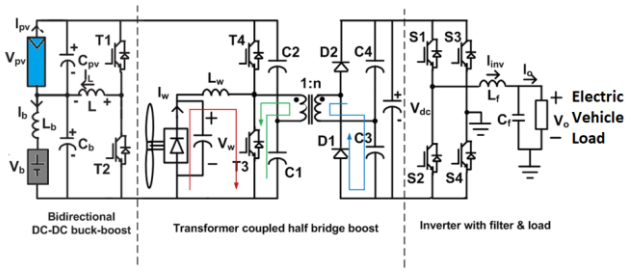

Figure 3: Negative conduction state (T3 - ON)

When the T3 switch is turned ON the inductor Lw connected in series to the DBR of the wind generator is charged from the PMSG power. During this mode, the current direction in the HFTF is negative charging the capacitor C1. The same direction of current is induced into the secondary side of HFTF conducting the diode D1 and charging the C3 in negative direction. However, the output voltage of the rectifier is DC voltage Vdc [13]. Now the voltage at the output DC terminal is with respect to the 'turns ratio' (n) in the

HFTF. In the next mode when T3 is turned OFF, T4 is turned ON due to the NOT gate action. When T4 switch is turned ON the direction of the current in the HFTF changes and also the inductor Lw discharges in series with the DBR of the wind generator. The positive conduction state with T4 ON with current direction is presented in figure 4.

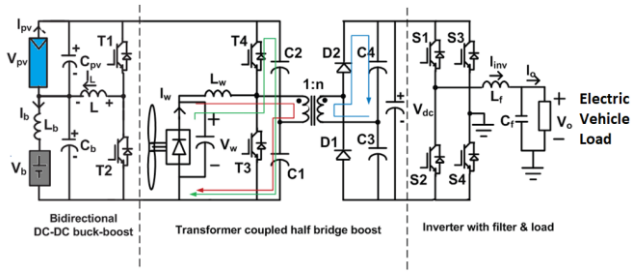

Figure 4: Positive conduction state (T4 - ON)

As observed in figure 4 the voltage from the DBR is added with the inductor Lw voltage (V_{LW}) and high voltage magnitude is generated. The current conducts in positive direction charging the capacitors C2 and C1. The positive voltage is induced to the secondary side of the HFTF and the diode D2 is conducting charging the capacitor C4. Now the voltage of the capacitor Cdc is increased to the boost voltage developed by the active bridge on the primary side [14]. The output DC voltage (V_{dc}) of the active half bridge converter is given as:

$$V_{dc} = \frac{nV_w}{1-D_w} = n\,(V_b + V_{pv}) \quad (1)$$

Here, Vw is the wind generator DBR voltage, Dw is the duty ratio of switch T3, Vb is the battery voltage and Vpv is the PV array voltage. In the bidirectional converter when T1 switch ON time is more than T2 switch the PV array power is stored into the battery pack through the inductors Lb and L. This mode occurs when the PV power is excess than the load demand. And when the T2 switch ON time is high than T1 switch the battery discharges through inductors Lb and L as the voltage of the battery mesh is now more than the PV array voltage. This mode occurs when the load demand is higher than the PV power generated [15]. As the battery discharges the power from the battery pack and the PV array are added and shared to the load. The current shared to the load through the inductor L is given as:

$$I_L = I_b + I_{pv} \quad (2)$$

The pair of switches T1 T2 and T3 T4 are controlled by individual controllers which tend to maintain the Vdc value at specified requirement of the load connected after the inverter.

3. Control structure design

Each converter in the proposed circuit topology has an individual controller which generated duty ratio for the switches T1 and T3. The other two switching signals for T2 and T4 are NOT gate pulses of the generated pulse T1 and T3 respectively. The switches of 'Bidirectional DC-DC buck boost converter' are operated as per the PV array power availability [16]. The charging and discharging of the battery pack is controlled by the ON and OFF times of the switches T1 and T2 [17]. The control design of the 'Bidirectional DC-DC buck boost converter' is presented in figure 5.

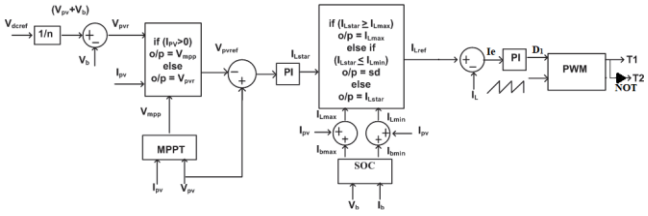

Figure 5: Control design of 'Bidirectional DC-DC buck boost converter'

In the given control design figure 5, there is voltage control loop and a current control loop which are defining the duty ratio D1 of the switch T1 [18]. As per the current control loop the duty ratio D1 is given as:

$$D_1 = \left(I_{Lref} - I_L\right)\left(k_{pi} + \int \frac{k_{ii}}{s}\right) \quad (3)$$

In the equation (3) the k_{pi} and k_{ii} are the proportional and integral gain of the PI current regulator of the current loop [19]. I_L is the measured inductor L current in the 'Bidirectional DC-DC buck boost converter' and the I_{Lref} is the reference inductor current selected as per the given expression below

$$I_{Lref} = \begin{cases} I_{Lmax}\,;\; If\; I_{Lstar} \geq I_{Lmax} \\ I_{Lmin}; If\; I_{Lstar} \leq I_{Lmin} \\ I_{Lstar};\; If\; I_{Lstar} > I_{Lmin} \end{cases} \quad (4)$$

The maximum, minimum ($I_{Lmax}\ I_{Lmin}$) and the reference current (I_{Lstar}) are given as per the PV current (I_{pv}), maximum and minimum battery reference value ($I_{bmax}\ I_{bmin}$) expressed as:

$$I_{Lmax} = I_{bmax} + I_{pv} \quad (5)$$

$$I_{Lmin} = I_{bmin} + I_{pv} \quad (6)$$

$$I_{Lstar} = \left(V_{pv} - V_{pvref}\right)\left(k_{pv} + \int \frac{k_{iv}}{s}\right) \quad (7)$$

Here, k_{pv} and k_{iv} are the proportional and integral gain of the PI voltage regulator, V_{pv} is the PV array voltage and V_{pvref} is the reference PV array voltage given as:

$$V_{pvref} = \begin{cases} V_{mp}; If\; I_{pv} > 0 \\ V_{pvr}; If\; I_{pv} = 0 \end{cases} \quad (8)$$

In the given expression (8) the V_{mp} is voltage at maximum power generated by P&O MPPT algorithm with feedback from Vpv and Ipv [20]. The V_{pvr} is the reference voltage expressed as:

$$V_{pvr} = n.V_{dcref} - V_b \quad (9)$$

From the given expression the final duty ratio D1 is compared to high frequency sawtooth waveform generating pulse for the switch T1 and NOT gate pulse to switch T2. The 'Bidirectional DC-DC buck boost converter' is now connected to a active half bridge converter with T3 and T4 switches [21] [22]. The controller for the active half bridge switches is presented in figure 6.

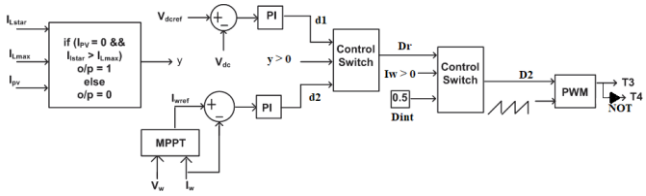

Figure 6: Control design of 'Active half bridge' converter

Similar to the previous controller the duty ratio D2 is selected as per the wind current I_w availability which is expressed as:

$$D_2 = \begin{cases} Dr; If\; I_w > 0 \\ 0.5; If\; I_w = 0 \end{cases} \quad (10)$$

The reference duty ratio Dr is also selected as per the I_{pv}, I_{Lstar} and I_{Lmax} values given as:

$$Dr = \begin{cases} d_1; If\ I_{pv} = 0\ AND\ I_{Lstar} > I_{Lmax} \\ d_2; If\ NOT\ (I_{pv} = 0\ AND\ I_{Lstar} > I_{Lmax}) \end{cases} \quad (11)$$

The duty ratio d_1 and d_2 are generated as per the reference values and wind voltage, current which are expressed as:

$$d_1 = \left(V_{dcref} - V_{dc}\right)\left(k_{p1} + \int \frac{k_{i1}}{s}\right) \quad (12)$$

$$d_2 = \left(I_{wref} - I_w\right)\left(k_{p2} + \int \frac{k_{i2}}{s}\right) \quad (13)$$

In the given expressions the I_{wref} is the reference wind current generated by P&O MPPT algorithm from feedback signals from wind generator voltage and current (V_w and I_w) [23]. The DC-AC single phase inverter need Sin reference signal for generating PWM pulses for the inverter switches (S1-S4). The reference Sin signal is generated by the required AC voltage magnitude, frequency and phase of the load. The control structure of the DC-AC single phase inverter is presented in figure 7.

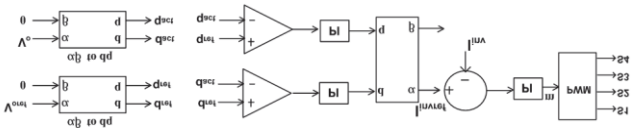

Figure 7: Control design of 'DC-AC single phase inverter

The reference voltage magnitude (m) is generated by the AC voltage regulator is expressed as:

$$m = \left(I_{invref} - I_{inv}\right)\left(k_{pac} + \int \frac{k_{iac}}{s}\right) \quad (14)$$

The inverter reference current (I_{invref}) is considered from the 'alpha' current component of the 'Inverse Parks' transformation. The dq current components are generated by the current regulators of the error dq components. The output voltage (V_o) of the inverter is achieved as per the reference required voltage (V_{oref}) set manually as per the load voltage demand [24]. The reference Sin signal generated is compared to high frequency triangular waveform generating PWM pulses for the switches S1 – S4 of the inverter.

4. Simulation analysis

The modeling of the proposed multi-input transformer coupled active bridge converter is done in Simulink environment with blocks considered from 'Electrical' subset of the Simulink library. Initially the PV array and battery circuit with the individual controller is modelled ensuring the output voltage generated is achieved as per requirement. The active half bridge is included later on at the DC link along with the wind farm and the controller for the converter. This two circuit are connected in parallel and the circuit analysis is carried out with a DC load connected on the rectifier side. Once the DC voltage at the output is stabilized the DC-AC single phase inverter is connected for compensating the AC load. The AC loads can be a two-wheel EV charging or a four wheeler EV charging which are presumed to be 5kW or 10kW respectively. The powers from the PV array, battery and wind generator are shared to the load operating either in MPPT or non-MPPT modes depending on load demand. The model is updated with the table 1 parameters given for each module of the proposed circuit.

Table 1: Module parameters

Module	Parameter
PV array	Manufacturer: Sunperfect Solar CRM295S156P-72 Vmp = 36.9V, Imp = 7.99A, Voc = 45.2V, Isc = 8.48A, Ns = 5, Np = 12, Ppv = 17Kw
Battery pack	Type: Lithium-Ion Vnom = 200V, Capacity = 60Ah, SOCint = 75%
PMSG	Pnom = 5kW, Tm = 10.2Nm, Vnom = 560Vdc, Nnom = 5000rpm, Rs = 0.18Ω, Ls = 0.825mH, Φ = 0.07145V.s, J = 0.00062kg.m2, F = 0.0003035N.m.s, p = 4, Base wind speed = 12m/s, Maximum power at base wind speed = 1pu, base rotational speed = 1.2pu
Bidirectional converter	Cpv = 1000µF, Cb = 100µF, L = 4mH, Lb = 1mH, Rigbt = 1mΩ, Vdcref = 400V, PI1: Kp = 0.06, Ki = 0.008, PI2: Kp = 0.01, Ki = 0.0023, fc = 10kHz
Active bridge	C1 = C2 = 200µF, Lw = 1mH, Cw = 3000µF, C3 = C4 = 400µF, Cdc = 12000µF, HFTF: n = 1, Pnom = 100kW, fnom = 10kHz, R1 = 0.01Ω, L1 = 1µH, R2 = 0.015Ω, L2 = 1.2µH, Lm = 500µH, Rm = 1000Ω, PI1: Kp = 0.001, Ki = 0.002, PI2: Kp = 0.002, Ki = 0.001, fc = 10kHz
Inverter	Rigbt = 1mΩ, Lf = 1mH, Cf = 1µF, Rload1 = 30kW, Rload2 = 20kW
Loads	Load 1 – EV battery charging 5kW Load 2 – EV battery charging 10Kw

The complete circuit is analyzed with different operating conditions by changing the solar irradiation, wind speed and load. The graphs of the active powers and the voltages of the modules are plotted for different operating conditions and are presented in the figures below.

Case 1: Load is varying while PV and Wind generating the power

In the first case the simulation is set with load variation at specific intervals of time and the stability of the circuit topology to the changes in observed. The figure 8 represents the active powers of the PV module, wind generator, battery and load. The simulation is run for 9s in which the load is changed from 5kW to 10kW during the period 3-6s.

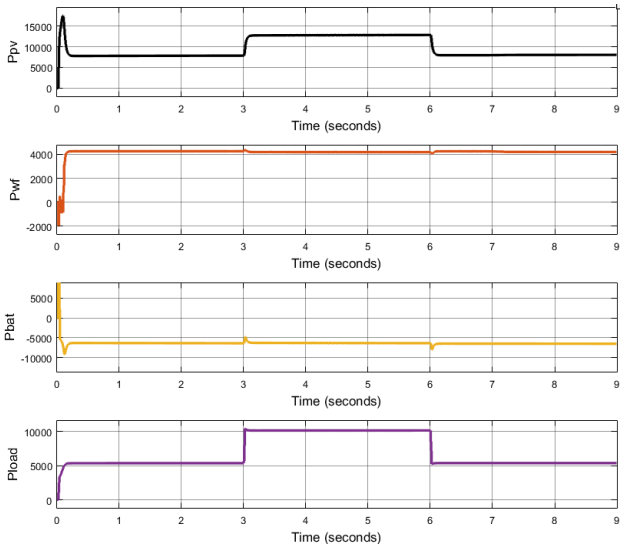

Figure 8: Active powers of the source and load during load variation

It is observed that the PV array which was previously working in non-MPPT mode changes to MPPT mode when the load is

increased. The PV power extraction increases from 7kW to 13kW once the load demand is increased. However, the wind power delivers constant 4kW and the battery is always charging by 6kW (negative direction represents charging) in any load demand condition.

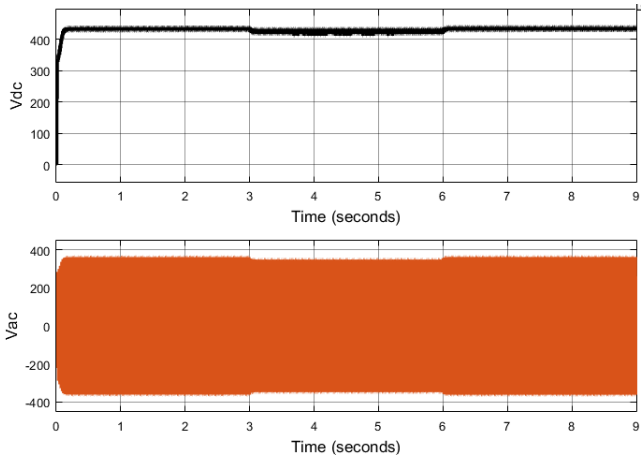

Figure 9: DC link voltage during load variation

Figure 9 shows the DC link voltage on the primary side of HFTF and the AC voltage at the load. It is observed that the DC link voltage and the AC voltage remain stable for any load change on the system validating the stability of the circuit.

Case 2: Wind power is not available but PV generating

In this case wind power is kept zero from initial simulation with only PV array and battery supporting the load. As presented in figure 10 the PV array provides 8kW with maximum power extraction and the battery discharges 2kW when the load demand is 10kW.

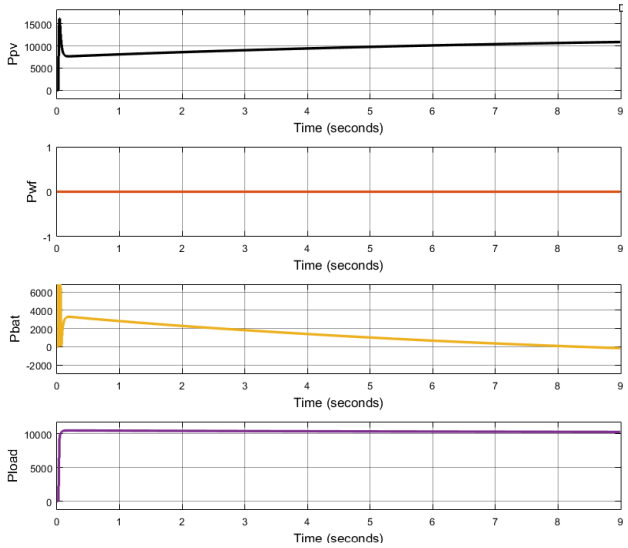

Figure 10: Active powers of the source and load during no wind power generation

From the figure 11 it is observed that the DC link voltage and the AC voltage are maintained stable even during no wind power generation and load variation. The DC volage tend to maintain at 400V.

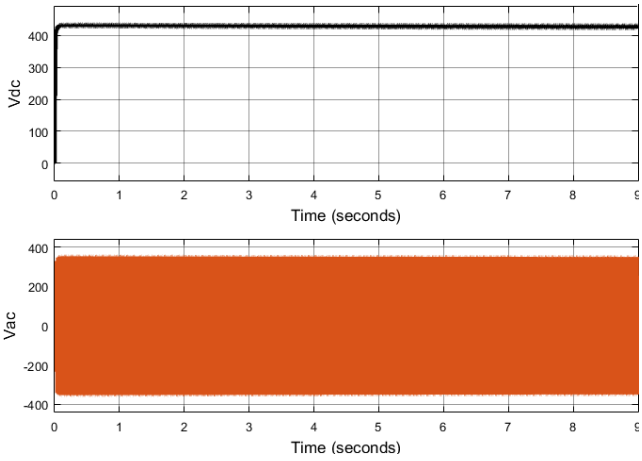

Figure 11: DC link voltage during no wind power generation

As the DC voltage is kept stable the AC voltage at the load side is also maintained stable at 230Vrms for any condition of the load.

Case 3: PV power is not available

In this case the PV power is dropped to zero at 4s with sudden change in the solar irradiation from 1000W/m^2 to 0W/m^2. The PV array power drops from 13kW to 0kW at 4s which is observed in figure 12.

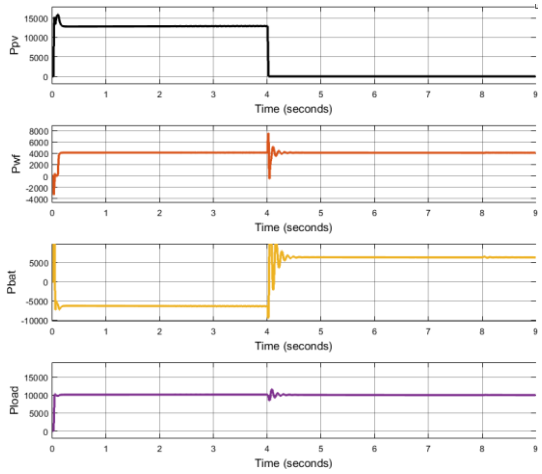

Figure 12: Active powers of the source and load during no PV power generation

It is observed that when the PV array power drops to zero the wind power is intact and delivers 4kW continuously. During the PV power availability, the battery is charging by 6kW which later on change to discharge mode with 6kW battery power delivering to the load at 4s.

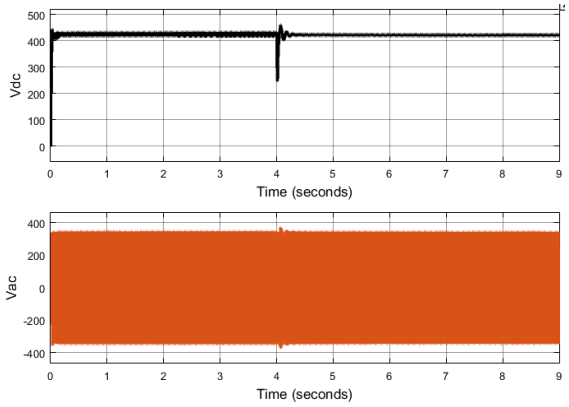

Figure 13: DC link voltage during no PV power generation

As per the presented figure 13 there is no change in the DC and AC voltages with the failure of PV source. The power supplied to the load is maintained at 10kW which is shared by wind generator and battery.

Case 4: Wind power and PV power is not available

In this case the PV array and wind generators completely fail at 3s and 6s with load completely depending on the battery unit. The 13kW PV array power and 4kW wind power comes to zero at 3s and 6s respectively drastically increasing the battery discharge power. The active power changes of the modules for this case are presented in figure 14.

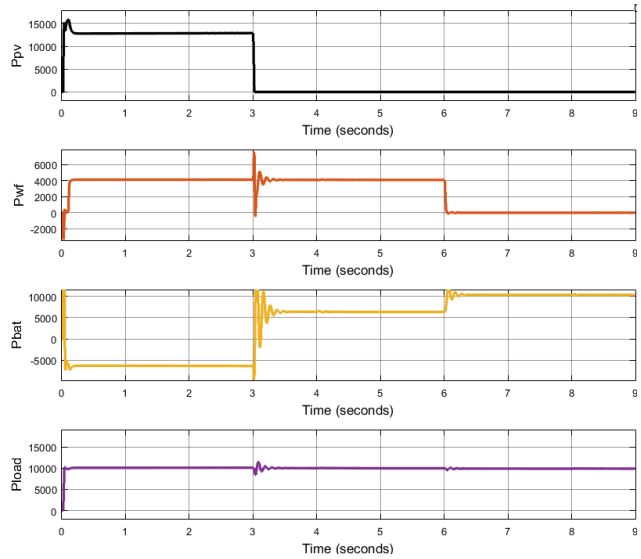

Figure 14: Active powers of the source and load during no PV and wind power generation

The battery power which is initially charging by 6kW changes to 6kW discharging at 3s when PV array fails and then jumps to 10kW discharging when wind generator fails at 6s. These conditions slightly impact the DC link voltage creating disruption at every change in PV and wind source powers.

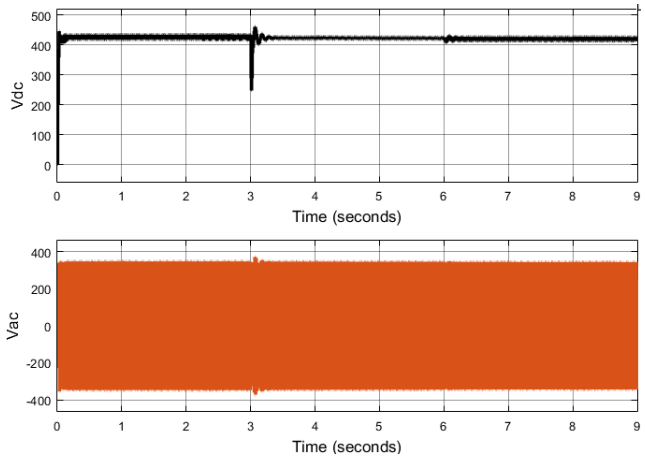

Figure 15: DC link voltage during no PV and wind power generation

As per figure 15 it is observed that the AC voltage is intact on the PV source and wind generator failures. The load is completely compensated by the battery pack with 10kW discharging to the load side with 240Vrms maintained throughout the simulation.

5. Conclusion

The modeling and testing of the proposed multi-input transformer coupled active bridge converter topology is done using MATLAB software in Simulink environment. The circuit is integrated with two renewable sources PV array and wind generator sharing power to the load with battery pack support. The standalone system is sustainable with no grid connection compensating the load connected to the circuit in any given condition. The circuit is controlled by individual controller which maintain the DC link voltage at specified value as per the requirement of the load. Maximum power extraction from the PV array and wind generator is achieved with the controllers adopting P&O MPPT algorithms. The circuit is tested with extreme load changes, solar irradiations and wind speeds observing the voltages on the DC side and AC side. It is validated that the circuit maintains the DC link voltage and AC voltage in the permissible range during these variations in the sources. The load is compensated either by the PV array power or wind generator power or battery power in any given operating condition.

References

[1] Erdiwansyah, Mahidin, Husin, H. et al. A critical review of the integration of renewable energy sources with various technologies. Prot Control Mod Power Syst 6, 3 (2021). https://doi.org/10.1186/s41601-021-00181-3

[2] Twaha, S., & Ramli, M. A. M. (2018). A review of optimization approaches for hybrid distributed energy generation systems: Off-grid and grid-connected systems. Sustainable Cities and Society, 41, 320–331. https://doi.org/10.1016/j.scs.2018.05.027.

[3] Van Hulle, F., Holttinen, H., Kiviluoma, J., Faiella, M., Kreutzkamp, P., Cutululis, N., … Ernst, B. (2014). Grid support services by wind and solar PV: A review of system needs, technology options, economic benefits and suitable market mechanisms: Synthesis report of the REserviceS project.

[4] Ruiz-Romero, S., Colmenar-Santos, A., Mur-Pérez, F., & López-Rey, Á. (2014). Integration of distributed generation in the power distribution network: The need for smart grid control systems, communication and equipment for a smart city — Use cases. Renewable and Sustainable Energy Reviews, 38, 223–234. https://doi.org/10.1016/j.rser.2014.05.082.

[5] Gevorkov, L.; Domínguez-García, J.L.; Romero, L.T.; Martínez, À.F. Modern MultiPort Converter Technologies: A Systematic Review. Appl. Sci. 2023, 13, 2579. https://doi.org/10.3390/app13042579

[6] T. -D. Duong, M. -K. Nguyen, Y. -C. Lim and J. -H. Choi, "An Active-Clamped Current-Fed Half-bridge DC-DC Converter With Three Switches," 2018 International Power Electronics Conference (IPEC-Niigata 2018 -ECCE Asia), Niigata, Japan, 2018, pp. 982-986, doi: 10.23919/IPEC.2018.8507795.

[7] Baloch, S.K.; Larik, A.S.; Mahar, M.A. Analyzing the Effectiveness of Single Active Bridge DC-DC Converter under Transient and Load Variation. Sustainability 2023, 15, 4773. https://doi.org/10.3390/su15064773

[8] Liu, Shengyong & Zhang, Xing & Guo, Haibin & Xie, Jun. (2010). Multiport DC/DC Converter for Stand-alone Photovoltaic Lighting System with Battery Storage. Electrical and Control Engineering, International

Conference on. 3894-3897. 10.1109/iCECE.2010.950.

[9] R. Liu, G. Zhou, Q. Tian and G. Xu, "Extendable Multiport High Step-Up DC–DC Converter for Photovoltaic-Battery Systems With Reduced Voltage Stress on Switches/Diodes," in IEEE Transactions on Industrial Electronics, vol. 70, no. 9, pp. 9123-9135, Sept. 2023, doi: 10.1109/TIE.2022.3206752.

[10] Paramasivam, M., Issac, A., Rakesh, N., & Subramaniam, S. (2023). Integrated battery management system employing multi-port DC/DC converter for standalone solar photovoltaic system. Energy Sources, Part A: Recovery, Utilization, and Environmental Effects, 45(3), 8239–8256. https://doi.org/10.1080/15567036.2023.2227157

[11] Shahriar Farajdadian, Amin Hajizadeh, Mohsen Soltani, "Recent developments of multiport DC/DC converter topologies, control strategies, and applications: A comparative review and analysis," Energy Reports, Volume 11, 2024, Pages 1019-1052, ISSN 2352-4847, https://doi.org/10.1016/j.egyr.2023.12.054.

[12] Hu, Yihua & Xiao, Weidong & Cao, Wenping & Ji, Bing & Morrow, D.J.. (2015). Three-Port DC–DC Converter for Stand-Alone Photovoltaic Systems. IEEE Transactions on Power Electronics. 30. 10.1109/TPEL.2014.2331343.

[13] Jagadeesh Ingilala, Indragandhi Vairavasundaram, "Investigation of high gain DC/DC converter for solar PV applications," e-Prime - Advances in Electrical Engineering, Electronics and Energy, Volume 5, 2023, 100264, ISSN 2772-6711, https://doi.org/10.1016/j.prime.2023.100264.

[14] Suresh K, Chellammal N, Bharatiraja C, Sanjeevikumar P, Blaabjerg F, Nielsen JBH. Cost-efficient nonisolated three-port DC-DC converter for EV/HEV applications with energy storage. Int Trans Electr Energy Syst. 2019; 29(10):e12088.

[15] Chen Y-M, Huang AQ, Yu X. A high step-up three-port DC–DC converter for stand-alone PV/battery power systems. IEEE Trans Power Electron. 2013; 28(11): 5049-5062.

[16] Lavanya A, Jegatheesan R, Vijayakumar K. Design of novel dual input DC–DC converter for energy harvesting system in IoT sensor nodes. Wirel Pers Commun. 2020; 117(4): 1-16.

[17] Varesi K, Hosseini SH, Sabahi M, Babaei E, Saeidabadi S, Vosoughi N. Design and analysis of a developed multiport high step-up DC–DC converter with reduced device count and normalized peak inverse voltage on the switches/diodes. IEEE Trans Power Electron. 2018; 34(6): 5464-5475.

[18] Yu Tang, Xingzhen Jiang, Yahu Gao, Coordinate control strategy for two-stage wide gain DC/DC converter, International Journal of Circuit Theory and Applications, 10.1002/cta.3304, 50, 9, (3136-3152), (2022).

[19] Liyin Bai, Zhidong Qi, Xuanhao Zhou, Kaihui Chu, Switch Capacitor–Based High Step-Up Three-Port DC–DC Converter for Fuel Cell/Battery Integration, International Journal of Circuit Theory and Applications, 10.1002/cta.4276.

[20] Almutairi, A.; Sayed, K.; Albagami, N.; Abo-Khalil, A.G.; Saleeb, H. Multi-Port PWM DC-DC Power Converter for Renewable Energy Applications. Energies 2021, 14, 3490. https://doi.org/10.3390/en14123490

[21] Qian, Z.; Abdel-Rahman, O.; Batarseh, I. An Integrated Four-Port DC/DC Converter for Renewable Energy Applications. IEEE Trans. Power Electron. 2010, 25, 1877–1887.

[22] Wang, Z.; Li, H. Integrated MPPT and Bidirectional Battery Charger for PV Application Using One Multiphase Interleaved Three-Port Dc-Dc Converter. In Proceedings of the 2011 Twenty-Sixth Annual IEEE Applied Power Electronics Conference and Exposition (APEC), Fort Worth, TX, USA, 6–11 March 2011; pp. 295–300.

[23] Su, G.-J.; Peng, F. A low cost, triple-voltage bus DC-DC converter for automotive applications. In Proceedings of the Twentieth Annual IEEE Applied Power Electronics Conference and Exposition, APEC 2005, Austin, TX, USA, 6–10 March 2005; pp. 1015–1021.

[24] Wu, H.; Chen, R.; Zhang, J.; Xing, Y.; Hu, H.; Ge, H. A Family of Three-Port Half-Bridge Converters for a Stand-Alone Renewable Power System. IEEE Trans. Power Electron. 2011, 26, 2697–2706.